Available online at www.sciencedirect.com
ScienceDirect
Procedia IUTAM 9 (2013) 3 – 15
Procedia IUTAM
www.elsevier.com/locate/procedia

IUTAM Symposium on Understanding Common Aspects of Extreme Events in Fluids

On the relation between small-scale intermittency and shocks in turbulent flows

Diego A. Donzis*, Shriram Jagannathan

Department of Aerospace Engineering, Texas A&M University, College Station, TX 77480, USA

Abstract

High Reynolds number turbulence is characterized by extreme fluctuations of velocity gradients which can interact with shock waves in compressible flows. While these processes are traditionally thought to happen at very disparate range of scales, both turbulence gradients as well as shock gradients become stronger as the Reynolds number increases. Our interest here is to investigate their relation in the high-Reynolds number limit. Our conclusion is that for intermittent turbulence with inertial range scaling exponents which grow more slowly than linear at asymptotically high orders, small-scale intermittency produces gradients which are commensurate with shocks. This result is interpreted in the context of shock-turbulence interactions where intermittency appears to be responsible, in part, for the holes observed in shocks from simulations and experiments. This effect is aided by the correlation between strong gradients and flow retardation ahead of the shock which is observed from analysis of our direct numerical simulation database of incompressible and compressible turbulence.

© 2013 The Authors. Published by Elsevier Ltd. Open access under CC BY-NC-ND license.
Selection and peer-review under responsibility of the School of Mathematical Sciences, University College Dublin

1. Introduction

An intrinsic feature of turbulent flows, especially at high Reynolds numbers is the appearance of extreme fluctuations in dissipation rates, enstrophy (vorticity squared), velocity gradients in general, velocity increments across small distances, among others [1]. This phenomenon, commonly referred to as internal intermittency, is present in both incompressible [2] and compressible flows [3–5]. The nature of these fluctuations can be seen in Fig. 1 where we show a normalized velocity gradient at an arbitrary plane from our DNS database of incompressible turbulence. As the Reynolds number increases, gradients (and hence dissipation) tends to become stronger in increasingly smaller regions of space, an effect also seen in the figure.

At the same time, in many applications turbulence could also interact with shock waves. A few examples include supernovae explosions, supersonic aerodynamics and propulsion, and inertial confinement fusion. Even in isotropic turbulence in a periodic domain without any external agent to generate conditions for a large-scale shock formation,

* Corresponding author.
E-mail address: donzis@tamu.edu

2210-9838 © 2013 The Authors. Published by Elsevier Ltd. Open access under CC BY-NC-ND license.
Selection and peer-review under responsibility of the School of Mathematical Sciences, University College Dublin
doi:10.1016/j.piutam.2013.09.002

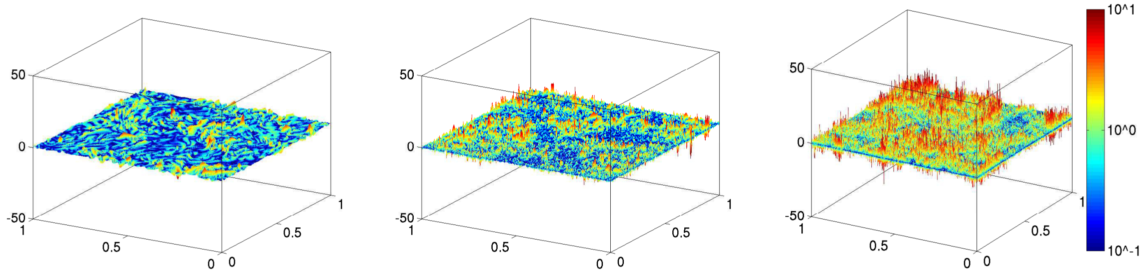

Fig. 1. Instantaneous velocity gradient (normalized by its rms values) on an arbitrary plane of the computational domain from our DNS database of incompressible turbulence at $R_\lambda \approx 140$ (a), 400 (b) and 1000 (c). In addition to changes in the spatial distribution of intense events as R_λ increases, the amplitude of such fluctuations (both positive and negative) increases as well (note values in vertical axes).

turbulence develops so-called shocklets [6–8] even at moderate turbulent Mach numbers ($M_t = u'/c$, where u' and c are the rms velocity and speed of sound respectively). Our focus, however, will be on the interaction of isotropic turbulence convected through a normal shock at Mach number $M = U/c$ (where U is the mean velocity of the incoming flow and c the mean speed of sound), a canonical problem which has received substantial attention [9] from theoretical [10–17], numerical [18–21], and experimental standpoints [22–25].

Most of the efforts mentioned above to understand shock-turbulence interactions, relied on treating the shock as a discontinuity, based on the assumption that the shock thickness is infinitely thin compared to all turbulence scales. However, this is, in many instances, not strictly justified [26]. (In the case of isotropic turbulence with shocklets it has even been suggested that the shocklet thickness is of the order of a few Kolmogorov length scales [7].) Moreover, most theoretical treatments further assumed an inviscid approximation and use linearized equations during the derivations. Results from such analyses, typically led to expressions which depend only on the shock Mach number M and not on the Reynolds number ($R_\lambda \equiv u'\lambda\rho/\mu$ where u' is the root-mean-square velocity, λ the Taylor microscale, and ρ and μ the mean density and viscosity of the turbulence before the interaction) or the turbulent Mach number (M_t). It has become clear, though, that the result of the interaction does depend on other characteristics of the incoming turbulence such as velocity and length scales [9]. It has also been observed that depending on the characteristics of the incoming flows, the interaction could be such that the nominally planar shock, is subjected to substantial deformation and could even develop “holes” through which properties do not undergo a quasi-discontinuous jump determined by Rankine-Hugoniot conditions [27, 18, 21]. Instead, multiple weak compression waves or even smooth transitions are observed along particular instantaneous streamlines. Interactions that present these characteristics are commonly referred to as in the “broken” regime. Although recent efforts [17] have successfully reproduced data in terms of low-order statistics of the distribution of gradients at the shock, a complete understanding of the scaling and origin of broken shocks, is still lacking.

Traditionally, turbulence processes and shock waves are assumed to happen at very disparate range of scales which is used to justify some strong simplifications widely used to study the interaction between them. However, because both, turbulence gradients and the shock gradient become steeper as the Reynolds number increases, it is of practical as well as fundamental importance to investigate whether turbulence gradients can become commensurate with shock gradients in high Reynolds number flows and have a first order effect on the shock structure. Investigating the plausibility of this scenario is the main thrust in the present work.

In [26] we have suggested that broken shocks may be possible if the shock thickness is comparable to the Kolmogorov length scale of the incoming turbulence. However, in subsequent work [17] we have studied the internal structure of the shock under turbulent conditions and suggested that milder conditions may lead to broken shocks too. In particular, locally sonic (or even subsonic) regions can create conditions where locally a shock is no longer possible. The resulting scaling does not depend on the Reynolds number. Here we extend our analysis to include dynamical aspects of the incoming flows. In particular, we will explore the influence of intermittency in the creation of broken shocks at high Reynolds numbers. As we will show, intermittency provides a viable mechanism for broken shocks which is further facilitated by local retardation of the flow ahead of the interaction.

2. Moments of velocity gradients

As noted in the introduction, extreme fluctuations in velocity gradients are an intrinsic feature of high-Reynolds numbers turbulent flows. These very intense gradients imply intense dissipation which at high Reynolds numbers, exhibit extreme fluctuations that could be several thousands times their mean value [28]. These are also related to the range of dissipative scales which are known to exist in intermittent turbulence that could be much smaller than the Kolmogorov scale [29].

In the context of turbulence interacting with a stationary shock, while linear superposition is clearly unjustified, intuitively it still seems possible that a very strong positive longitudinal gradient $\partial u/\partial x$ can interact with the negative mean gradient of the shock to produce local topological changes in the flow which may result in smooth transitions or multiple weaker compression waves. It is natural to think that this interaction may be effective, though, only if turbulence gradients are commensurate to shock gradients. Estimating the conditions under which this is possible is the main objective of the next sections.

2.1. Shock gradient

Laminar solutions to the problem of a one-dimensional shock at Mach number M are well known [30]. In the case of an inviscid approximation (or far away from the shock), the conditions upstream and downstream of the shock are completely determined by M. If viscosity is taken into account, one can still solve the Navier-Stokes equations numerically to obtain the structure of the shock. This has been extensively compared to experimental measurements [e.g. 31] in both monoatomic and diatomic gases and the general conclusion is that Navier-Stokes equations provide a reasonable approximation of the shock structure for values of M in the range $1.0-2.0$ depending on the accuracy needed. For strong shocks the Navier-Stokes equations result in inaccurate predictions of shock thicknesses [e.g. 32]. In particular, the predicted thickness is smaller (and gradients larger) than what is observed in experiments. Recent work, however, suggests that the inclusion of additional stress terms appear to improve the predictions [e.g. 33, 34, 32].

While further consequences of these inaccuracies will be discussed in the context of the results obtained below, here we focus on the classical analytical solution for weak shocks [35] to obtain first order estimates of the quantities involved. In particular, if we use u_x to denote $\partial u/\partial x$ (both u and x are in the streamwise direction) one can write the maximum gradient at the shock, $\hat{u}_x^s$ (caret represents the maximum velocity gradient and the superscript s is used to denote shock gradients), as [30]

$$\hat{u}_x^s = k[u]^2, \tag{1}$$

where $k = -(\gamma+1)/8D$, $D = (\mu/\rho)(4/3+\mu_v/\mu+(\gamma-1)/Pr)$, γ is the ratio of specific heats, μ_v is the bulk viscosity, Pr is the Prandtl number and, $[u]$ is the velocity jump across the shock as obtained from Rankine-Hugoniot conditions.

This relation can also be written in terms of the mean Mach number M by noting that the velocity jump is given by $[u] = 2c/(\gamma+1)(M-1/M)$. We will also assume, for simplicity in the argument, that $D \approx \mu/\rho = \nu$ which is valid for zero bulk viscosity (or constant μ_v/μ) and constant Prandtl number. For example, for $\mu_v = 0$, $\gamma = 1.4$ and $Pr \approx 0.72$ the proportionality constant is not far from unity. Thus we can write,

$$\hat{u}_x^s \approx \frac{\rho c^2}{\mu}\left(M-\frac{1}{M}\right)^2. \tag{2}$$

It will be convenient to recast this expression also in terms of $\Delta M = M-1$ [26, 17]. Furthermore, for future use, we note that we can expand Eq. (2) in series of ΔM. To leading order, the term in parenthesis scales as ΔM both at low and high values of ΔM (with different $O(1)$ prefactors). Thus, we could write

$$\hat{u}_x^s \approx \frac{\rho c^2}{\mu}\Delta M^2, \tag{3}$$

if we drop all order-unity prefactors. Furthermore, in terms of non-dimensional numbers, Eq. (3) can be easily recast in the following form

$$\hat{u}_x^s \approx \frac{1}{T}\frac{R_L}{{M_t}^2}\Delta M^2, \tag{4}$$

where $T \equiv L/u$ is the so-called eddy-turnover time and $R_L \equiv \rho u L/\mu$ is the large-scale Reynolds number which is also related to the Taylor Reynolds number through the well known formula $R_L \sim R_\lambda{}^2$.

2.2. *Turbulence gradients*

While the origin of the strong fluctuations in velocity gradients is still an open problem, their effect is commonly linked to the so-called anomalous scaling of structure functions [2] which are defined as moments of velocity increments over a distance r: thus $S_n(r) \equiv \langle \Delta_r u^n \rangle = \langle [u(x+r) - u(x)]^n \rangle$ is the longitudinal structure function of order n, where the velocity u is in the direction of the separation r and angular brackets represent an ensemble average.

While our interest is in velocity gradients, much more effort has been devoted to measure structure functions, in part because of the relative ease in which they can be obtained in experiments and numerical simulations as well as accuracy issues when compared to, for example, the full dissipation rate. This is especially so when high-order moments are considered. The relation between the scaling of velocity gradients and structure functions, however, has been recognized for a long time [2]. In fact, a number of theoretical results predicting the scaling of dissipation or velocity gradients have been developed assuming the scaling of structure functions is known [36, 37]. This is the approach we will follow here as well.

The anomalous scaling of structure functions can be quantified by their departure from the self-similar scaling of Kolmogorov 1941 (K41 for short) which predicts,

$$S_n(r) = C_n(r\langle\varepsilon\rangle)^{n/3}, \tag{5}$$

in the inertial range of scales, $\eta \ll r \ll L$ where $\eta \equiv (\nu^3/\langle\varepsilon\rangle)^{1/4}$ and L are the Kolmogorov and integral length scales of the flow. The relation between them is given by $\eta/L \sim R_\lambda{}^{-3/2}$. In Eq. (5), C_n is a flow-dependent constant, and $\langle\varepsilon\rangle$ is the average energy dissipation rate. It has become clear, however, that due to intermittency, exponents depart from K41 predictions and that this effect increases with the order of the moment considered [2]. Instead of Eq. (5), it is found that structure functions scale as

$$S_n(r) \sim \left(\frac{r}{L}\right)^{\zeta_n}, \tag{6}$$

with $\zeta_n < n/3$ for $n > 3$. As we will see below, our interest is in the asymptotic behavior of ζ_n for large n.

For very small separations, the first term in a Taylor expansion of $S_n(r)$ can be taken and the resulting expression is

$$S_n(r) = r^n \langle u_x^n \rangle. \tag{7}$$

The range of scales where Eq. (7) is valid, is usually called the analytic range. This range is observed as a plateau at small scales if structure functions are normalized as $S_n(r)/r^n$ and plotted against r. An example from well-resolved DNS [28] at $R_\lambda \approx 140$ is shown in Fig. 2.

The matching of Eqs. (6) and (7) presents a basis for the relation between scaling exponents of structure functions and moments of velocity gradients. While some early work assumed the matching scale between analytical and inertial ranges to be close to the mean Kolmogorov length scale [39, 40], later work [e.g. 36] assumed this matching scale to be determined by the *local* scaling exponents of structure functions within the so-called multifractal formalism [see 29, for more details]. More recently Yakhot and Sreenivasan [37, 38] attempted to stay closer to the governing equations and obtained specifically these order-dependent matching scales. It was found that different orders require different matching separations [41, 28]. These scales, which behave as $R_\lambda{}^{3/2+2/(\zeta_n-\zeta_{n+1}-1)}$ when normalized by the mean Kolmogorov scale, are also indicated in Fig. 2.

Because, as we will see momentarily, extreme events are governed by the asymptotic behavior of scaling exponents at large n where obtaining reliable data from experiment and simulations is extremely challenging, we have examined the predictions of both, the recent theory of Yakhot-Sreenivasan [37] (YS for short) and the multifractal model (MF for short) with the hope that some consistently is found. This is indeed the case as we show next.

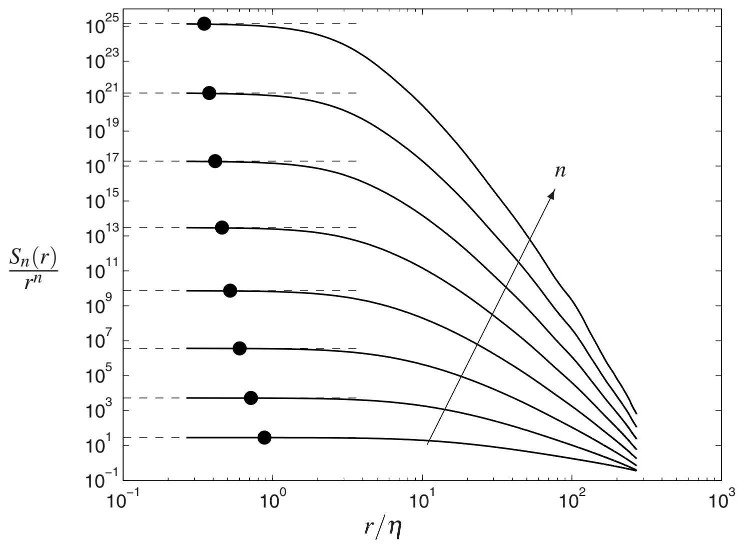

Fig. 2. Scaling of normalized longitudinal structure functions $S_n(r)/r^n$ for n =2, 4, 6, 8, 10, 12, 14 and 16, from a highly resolved simulation at $R_\lambda \approx 140$ and 2048^3 resolution [28]. Moments of velocity gradients $\langle u_x^n \rangle$ are shown as dashed lines. Solid circles denote the order-dependent dissipative scales proposed by Yakhot and Sreenivasan [38].

2.2.1. *Velocity gradients according to YS*

Following the theoretical work of Ref. [37] we can write the moments of velocity gradients as $\langle u_x^n \rangle \sim {R_L}^{m_n}$ with $m_n = (\zeta_n - n)/(\zeta_n - \zeta_{n+1} - 1)$. Velocity gradients can be conveniently normalized with the result for $n = 2$, namely, $\langle u_x^2 \rangle^{n/2} \sim {R_L}^{m_2 n/2}$ where $m_2 = 1$ due to dissipative anomaly [42]. We can then write $\langle u_x^n \rangle / \langle u_x^2 \rangle^{n/2} \approx {R_L}^{m_n - m_2 n/2} \approx {R_\lambda}^{2m_n - n}$ where the relation $R_L \approx {R_\lambda}^2$ has been used. Since we also have $\langle u_x^2 \rangle \sim \langle \varepsilon \rangle / \nu$, the moments can then be written as

$$\langle u_x^n \rangle \approx \tau_\eta^{-n} {R_\lambda}^{2m_n - n}, \tag{8}$$

where $\tau_\eta \equiv (\nu/\langle \varepsilon \rangle)^{1/2}$ is the Kolmogorov time scale, charactersitic of the small scales of motion. The strongest turbulence gradients can now be obtained by taking the $n \to \infty$ limit of $\langle u_x^n \rangle^{1/n}$ as follows

$$\begin{aligned} \hat{u}_x^t &\approx \lim_{n\to\infty} \left\{ \left[\tau_\eta^{-n} {R_\lambda}^{(2m_n - n)} \right]^{1/n} \right\} \\ &\approx \tau_\eta^{-1} {R_\lambda}^{s_\infty}, \end{aligned} \tag{9}$$

where $s_\infty = \lim_{n\to\infty} s_n = \lim_{n\to\infty}(2m_n/n - 1)$ is given explicitly in terms of inertial range scaling exponents as

$$s_\infty = \lim_{n\to\infty} \left[\frac{2}{n} \frac{\zeta_n - n}{\zeta_n - \zeta_{n+1} - 1} - 1 \right]. \tag{10}$$

The notation $\hat{u}_x^t$ in Eq. (9) is used to emphasize the distinction between the maximum velocity gradients in the incoming turbulence (superscript t) and that at the shock in Eq. (1) (superscript s).

2.2.2. *Velocity gradients according to MF*

The main idea of the multifractal model is that velocity increments possess a *local* scaling exponent h such that $\Delta_r u \sim r^h$ on a set of fractal dimension $D(h)$. The consequences of the multifractal model for velocity gradients were first put forth by Nelkin [36] who pointed out that one can write $u_x \sim l^{h-1}$ for l in the analytic range which is determined by $l \sim \nu^{1/(1+h)}$. By using a steepest descent argument one can find [see, Ref. 29, for details] that moments of velocity gradients are given by

$$\langle u_x^n \rangle \approx \tau_\eta^{-n} {R_\lambda}^{2d_n}, \tag{11}$$

with $d_n = p(n) - 3n/2$ and $p(n)$ is the value of p that satisfies $\zeta_p = 2n - p$ for a given n and scaling exponents ζ_p. Again, the strongest gradients are then found by taking the limit $\lim_{n\to\infty}\langle u_x^n\rangle^{1/n}$. The result is

$$\hat{u}_x^t \approx \tau_\eta^{-1} {R_\lambda}^{s_\infty}, \tag{12}$$

where s_∞ is now given by

$$s_\infty = \lim_{n\to\infty}\left(\frac{2p(n)}{n} - 3\right). \tag{13}$$

While the scaling of moments appear to be different for the two theoretical approaches (Eqs. (10) and (13)), as we show below, the scaling of extreme events is actually similar.

3. Comparison between turbulence and shock gradients: Reynolds number scaling

3.1. Ratio of strongest turbulence and shock gradients

We are now interested in comparing the strongest gradients in the incoming turbulence with the gradient at the shock. Using Eq. (4) and either Eq. (9) or (12) , we can now compute the ratio between them, K_u, as

$$K_u \equiv \frac{\hat{u}_x^t}{\hat{u}_x^s} \approx \frac{T}{\tau_\eta}\frac{{R_\lambda}^{s_\infty}}{R_L \Delta M^2 {M_t}^{-2}} \approx \frac{{M_t}^2}{R_\lambda \Delta M^2}{R_\lambda}^{s_\infty}. \tag{14}$$

where, for the last equality, we have used the well-known result $T/\tau_\eta \approx R_\lambda$ and $R_L \approx {R_\lambda}^2$. This can also be written in terms of the parameter $K = M_t/{R_\lambda}^{1/2}\Delta M$ which was suggested in [26] to provide a universal description of so-called amplification factors of velocity fluctuations across the shock. It is also possible to show that $K \approx \delta_l/\eta$ where δ_l is the laminar shock thickness [17]. The result is

$$K_u \approx K^2 {R_\lambda}^{s_\infty}. \tag{15}$$

which shows that while the mean Kolmogorov length scale may be larger than the laminar shock thickness (i.e. $K < 1$), depending on the value of s_∞, small-scale intermittent activity could be as strong as the shock at high Reynolds numbers. Quantitatively, if $K_u \gtrsim 1$ then the turbulence velocity gradients are comparable or larger than the shock gradient and a local disruption of the shock seems plausible. However, we also note that for such events to be possible, K_u does not necessarily need to be much greater than unity; even if $K_u \sim O(1)$ (or even smaller) turbulence can still create large perturbations in the shock. As we will see below, this effect is aided by retardation of the flow ahead of the shock.

Clearly, from Eq. (15), if $s_\infty > 0$, then for fixed K, K_u grows unbounded as the Reynolds number increases and local topological changes (“holes” in the shock) due to strong intermittent events, become more likely. To examine more closely the conditions under which intermittency is a viable route for broken shocks as different parameters are changed, we rewrite Eq. (15) as

$$K_u \approx \frac{{M_t}^{(3+s_\infty)/2}}{{R_c}^{(1-s_\infty)/2}\Delta M^2} \tag{16}$$

where $R_c = \rho c L/\mu$ [17]. The advantage of using these parameters is that u, for example, is reflected in only one nondimensional group (M_t) instead of two (M_t and R_λ). This also helps clarify the differences between increasing u or L, for example, as opposed to simply increasing R_L.

Eq. (16) now clearly shows that increasing u will lead to $K_u \gtrsim 1$ regardless of the value s_∞ making intermittency effects more predominant. The behavior with R_c, on the other hand, is more interesting since it can, in principle, present different qualitative trends depending on how s_∞ compares to unity.

To estimate s_∞, we note that although a number of theoretical results have been proposed for ζ_n for realistic turbulence with anomalous scaling [29], all comparisons with experimental and numerical data were necessarily performed for low to moderate values of n where models typically agree reasonably well [29, 41]. However, as

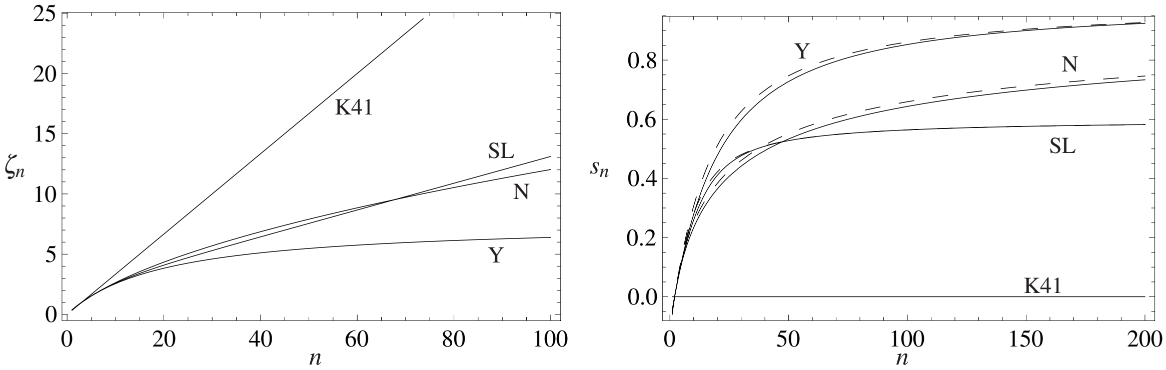

Fig. 3. Scaling exponents of (a) structure functions ζ_n and (b) moments of velocity gradients s_n. The notation corresponds to K41: Kolmogorov [44]; N: Novikov [45]; Y: Yakhot [46]; SL: She-Leveque [43]. The exponents shown in part (b) are computed from Eq. (10) (solid) and Eq. (13) (dashed), which correspond to YS and MF theories, respectively.

we pointed out above, the relevant information is contained in the asymptotic behavior of ζ_n and not in the specific functional form for small n. Furthermore, different models are based on (sometimes completely) different physical pictures of the mechanisms for extreme invents in high-Reynolds number turbulence.

Thus, we now consider particular expressions for ζ_n which are shown in Fig. 3.1(a) for values of n well beyond what can be reliably estimated from experiments and simulations. For non-intermittent turbulence K41 provides $\zeta_n = n/3$ which, by using Eq. (10), yields $s_\infty = 0$. This result is expected since fluctuations in velocity gradients are neglected in the theory. As expected, the same exponent $s_\infty = 0$ is obtained when $\zeta_n = n/3$ is used with the MF result Eq. (13). A more sophisticated approach that accounts for anomalous scaling is the She-Leveque model [43] which is based on a hierarchy of dissipative structures and results in $\zeta_n = n/9 + 2[1-(2/3)^{n/3}]$. It is easy to see that ζ_n scales as $2+n/9$ for large n which, therefore, results in $s_\infty = 3/5$ from either Eq. (10) or Eq. (13).

Now consider Yakhot's result [46] $\zeta_n = (1+3\beta)n/3(1+\beta n)$. In the high-$n$ limit, ζ_n approaches a constant and thus, $s_\infty = 1$ using either Eq. (10) or Eq. (13). Nelkin [47] noted that using Novikov models [45] one can write $\zeta_n = [1+n(c_N/3)]^{1/2}/[(1+c_N)^{1/2}-1]$ where c_N is a constant. For very large n, ζ_n scales as $\sim \sqrt{n}$ and s_∞ will also tend to 1. More generally, it is possible to show from Eq. (10), for example, that the result $s_\infty = 1$ is valid for any model that predicts an asymptotic growth of ζ_n slower than n, which obviously includes those predicting the saturation of scaling exponents, at large n. (Saturation of scaling exponents has been observed [48] also for density and entropy fluctuations in simulations of weakly compressible turbulence which was attributed to "front-like" structures in the flow.)

The asymptotic behavior of ζ_n has been discussed before. For example, [46] argues that a linear asymptotic regime $\zeta_n \propto n$ in the high-n limit it is rather improbable (as exhibited by K41 and the She-Leveque model). This conclusion is based on the structure of the governing equations for moments of velocity increments (structure functions) of arbitrary order and the probability density functions of those velocity increments. On the other hand, Yakhot suggests that saturation of exponents $\zeta_n \to const$ is possible for a wide class of probability densities functions. Nelkin [36] has also studied the asymptotic behavior of ζ_n in the context of the Novikov and She-Leveque models. While experimentally indistinguishable from each other for $n < 100$ (see Fig. 3.1(a)), the underlying dynamical assumptions are quite different and some of the consequences can be seen in the exponents s_n seen in Fig. 3.1(b). The fact that She-Leveque presents a linear scaling at large n, can be traced back to the assumption behind the most intense events of the locally averaged dissipation rate which are assumed to scale according to K41 [36]. Thus the asymptotic linear scaling appears to be a residual effect of such an assumption.

We now turn again to Eq. (16) in the context of broken shocks. Under K41, we saw that $s_\infty = 0$ and, therefore, $K_u \approx K^2$. Since typically $K < 1$ [see e.g. 26], turbulence gradients are not expected to be comparable to the shock gradient, which is consistent with a thin shock interacting with non-intermittent turbulence. If instead, $0 < s_\infty < 1$, an increase in the Reynolds number R_c will lead to a decrease in K_u and a broken shock through intermittency mechanisms is less likely. Eq. (16) also allows us to see that an increase in the integral length scale of the turbulence L will have the opposite effect than increasing the turbulence fluctuations u, a result that is not readily seen if R_λ is used instead of R_c. However, as argued above, there are reasons against a linear asymptotic scaling of ζ_n, making $s_\infty = 1$ the most plausible result. In that case the Reynolds number dependence disappears in Eq. (16) and

$$K_u \approx {M_t}^2/\Delta M^2. \tag{17}$$

This is the direct result of small-scale intermittent events having the same scaling as the shock itself. In Sec. 5 we show that this can also be interpreted in terms of the most singular structures leading to very fine structures.

The conclusion is, thus, that for non- and weakly-intermittent turbulence characterized by scaling exponents of the form $\zeta_n \sim n$ for asymptotically large n, broken shocks are likely when K is large [26] (see Eq. (15) with $s_\infty = 0$). For strongly intermittent (and more realistic) turbulence characterized by scaling exponents with asymptotic behavior weaker than $\sim n$, on the other hand, broken shocks are likely when $M_t/\Delta M$ is not too small (see Eq. (16) with $s_\infty = 1$), a situation of practical interest. The significance of this result is that even at moderate values of $M_t/\Delta M$, intermittency may become a major factor in broken shocks, independent of Reynolds numbers.

We note that although Eq. (17) turns out to have no Reynolds number dependence, its derivation is based on moments of velocity gradients and increments approaching their high-Reynolds number asymptotic scaling state. It seems, however, that these scaling exponents are already seen at very low Reynolds numbers [41].

4. Regime of the interaction

As mentioned above, the interaction of isotropic turbulence and a normal shock could be in different regimes depending on whether the shock remains a sharp gradient across the entire surface or it is greatly distorted leading to very smooth compressions or multiple compression waves along individual streamlines. These have been referred to as wrinkled and broken (or peaked and rounded) regimes [27, 21] respectively. Since their definition has been typically based on visual inspections of instantaneous profiles or contours of pressure or density, in Ref. [26] we have suggested that the parameter K can be used to quantitatively assess the characteristics of the interaction. More recently [17] we have proposed another mechanism based on locally subsonic regions under which a stable shock is not possible and appears to agree well with results of numerical simulations and is briefly described below. Here, we examine these results in light of our findings of the scaling of intermittent gradients.

The mechanism suggested in [17] assumes that the incoming turbulent velocity field is described by Gaussian statistics which is, in general, a good approximation [49]. Note that this assumption is needed only for the one-point PDF of the velocity component normal to the shock and, therefore, does not preclude intermittency effects. Since at any given location across the shock surface the local Mach number is given by $1+\Delta M+\tilde{m}$, where $\tilde{m}$ is the instantaneous Mach number defined as $\tilde{u}/c$ ($\tilde{u}$ is the instantaneous velocity component normal to the shock surface), the probability of finding subsonic velocities is given by $P_S \equiv P(\tilde{m} < -\Delta M)$. For a Gaussian velocity field, one can then obtain [17] $P_s = (1-\mathrm{erf}(\sqrt{3/2}\Delta M/M_t))/2$ where erf(.) is the error function. For later comparison, we note that the likelihood of broken shocks scales with the parameter $M_t/\Delta M$.

In previous sections we have argued that intermittent gradients can cause local disruptions of the shock and could thus lead to a broken regime when $K_u \gtrsim 1$. Here we note that there are two additional factors that could make intermittency effects even more preeminent in shock-turbulence interactions. First, in Eq. (14), K_u may be underestimated since the shock gradient $\hat{u}_x^s$ has been calculated assuming that the incoming flow is characterized by ΔM. However, since the Mach number at the shock surface locally includes also turbulence fluctuations the appropriate Mach number is $1+\Delta M+\tilde{m}$ [17]. Thus, due to fluctuations, wider shocks may appear in regions where the local Mach number is close to unity, or equivalently, $\Delta M+\tilde{m}$ is small. If the most negative value of $\tilde{m}$ is some fraction α of M_t we obtain, for $s_\infty = 1$, $K_u \approx {M_t}^2/(\Delta M-\alpha M_t)^2 \approx ({M_t}^2/\Delta M^2)/(1-\alpha M_t/\Delta M)^2$. For fluctuations of, say, four times the turbulent Mach number (i.e. $\alpha = 4$) then K_u will be much larger than that predicted by Eq. (15) even for moderate values of $M_t/\Delta M$, say, 0.25 which is lower than that required for significant subsonic regions according to the arguments in [17]. We must note, however, that this scenario will require both an extreme turbulence velocity gradient (as suggested above) combined with a local negative velocity fluctuation (as suggested in Ref. [17]). To assess the likelihood of such an event, joint statistics of velocity and its gradient are needed.

We have analyzed our DNS database of forced isotropic incompressible turbulence (e.g. Ref. [28], where details of the simulations can be found), to assess whether such a correlation exists, supporting the scenario of a combination of large velocity gradients and relatively low speeds. The results are seen in Fig. 4 where we show the conditional expectation of the square of (normalized) longitudinal velocity gradients (i.e. $u_x^2/\langle u_x^2\rangle$) given values of the velocity component in the same direction, normalized by the rms (i.e. $\tilde{u}/u$) at two Reynolds numbers ($R_\lambda \approx 140$ and 400) higher than those achievable for current shock-turbulence interactions since our main interest is in high-Reynolds number flows. Clearly, regions of high (positive and negative) velocities are correlated with larger values of velocity gradients. To test the effect of compressibility, we have also performed DNS of forced isotropic compressible turbulence at comparable conditions ($R_\lambda \approx 160$) but at $M_t \approx 0.3$.[1] We can see that the correlation between large gradients and large (positive and negative) velocities is maintained, at least, at these Reynolds and Mach numbers.

The second factor that could make intermittency effects on the shock more severe than one-point statistics may indicate, is the fact that intense events tend to cluster in space [50, 51]. In such a case, the shock will be subjected to a train of strong gradients whose cumulative effect, as they are advected to the shock, could destroy the shock locally.

It is interesting to note that due to intermittency broken shocks appear when $M_t/\Delta M$ increases (Eq. (17)) which represent the same scaling, though based on completely different physical mechanisms, than that predicted for a Gaussian velocity field producing subsonic local conditions [17]. While the former is a high-Reynolds number phenomenon, the latter is based on kinematics independent of the Reynolds number.

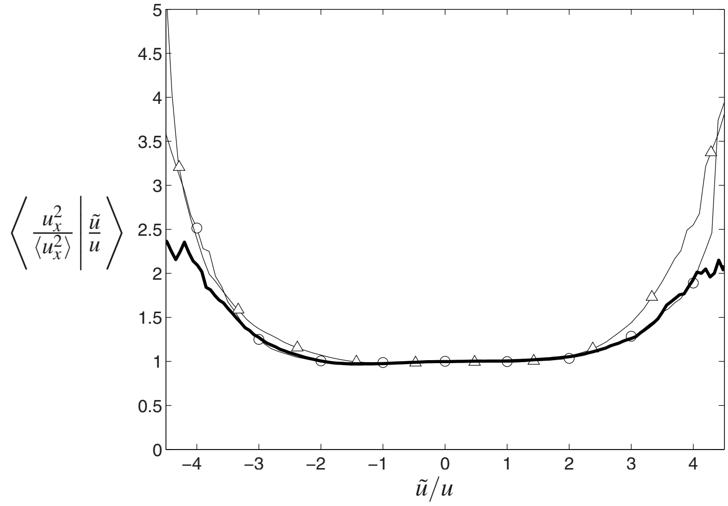

Fig. 4. Conditional mean of normalized velocity gradients given normalized velocity from direct numerical simulations of incompressible turbulence at $R_\lambda \approx 140$ (circles) and 400 (triangles) and compressible turbulence at $R_\lambda \approx 160$ and $M_t \approx 0.3$ (thick line with no symbol).

We finally make a note about the generality of the preceding results. The estimate of the shock gradient in Eq. (3) can be derived from Navier-Stokes equations for small values of ΔM, thus limiting, in principle, its applicability to weak shocks. However, if intermittent gradients are accompanied by negative velocity fluctuations creating close-to-sonic regions, then at those locations the Mach number will not be much different than unity in which case, Eq. (3) is locally a good approximation. It is also known that for strong shocks the Navier-Stokes equations result in inaccurate predictions of shock thicknesses. In particular, the predicted thickness is *smaller* than what is observed in experiments [31] (though the inclusion of bulk viscosity appear to improve the predictions [33]). Therefore, at high ΔM, shock gradients will be smaller than predicted by Eq. (3) resulting in a larger K_u. Intermittency appears then to be even more effective when strong shocks not captured accurately by Navier-Stokes solutions are considered.

[1] The details of the simulations will be presented elsewhere we note here their main characteristics. Discretization is based on tenth-order compact schemes in space and third-order Runge-Kutta in time and grid-convergence studies have been performed. The forcing scheme is stochastic similar to the one in incompressible simulations but energy is removed in the energy equation to maintain the mean temperature constant and achieve a stationary state.

5. A multifractal interpretation in terms of length scales

The similar scaling of turbulence and shock gradients in intermittent turbulence can also be interpreted in terms of length scales within the multifractal formalism. Since intermittent turbulence possess scales much smaller than the mean Kolmogorov scale, η, it has become increasingly clear [52, 53] that it is more appropriate to determine the local Kolmogorov scale $\eta' = (\nu^3/\varepsilon)^{1/4}$ using instantaneous values of the dissipation, ε. The smallest scale, then, is obtained as

$$\eta_{min} = (\nu^3/\varepsilon_{max})^{1/4} \tag{18}$$

where ε_{max} is the largest value of dissipation. To estimate ε_{max}, one can consider ε_r, the local average of dissipation over a linear dimension r, which according to the MF model scales as

$$\varepsilon_r \approx \langle\varepsilon\rangle\,(r/L)^{\alpha-1} \tag{19}$$

where α is the singularity exponent, itself a random variable. At the corresponding local Kolmogorov scale η' one would expect the local Reynolds number $R_r = \varepsilon_r^{1/3} r^{4/3}/\nu$ to be $O(1)$ when r corresponds to the local dissipation scale, η'. This condition is equivalent to Eq. (18).

From $R_r \approx 1$ and the well-know result $\langle\varepsilon\rangle \sim u^3/L$ we can now obtain

$$\eta'/L \approx R_\lambda{}^{-6/(3+\alpha)} \tag{20}$$

or in terms of the mean Kolmogorov scale

$$\frac{\eta'}{\eta} \approx R_\lambda{}^{-(3/2)(1-\alpha)/(3+\alpha)} \tag{21}$$

The smallest dissipative scale would then correspond to the smallest scaling exponent α_{min} which, in turns, corresponds to the strongest fluctuations in dissipation according to Eq. (19):

$$\frac{\eta_{min}}{\eta} \approx R_\lambda{}^{-(3/2)(1-\alpha_{min})/(3+\alpha_{min})} \tag{22}$$

We now want to compare η_{min} with the shock thickness δ_l. Since the ratio of the latter with the mean Kolmogorov scale is given by $\delta_l/\eta = K$ with $K = M_t/R_\lambda{}^{1/2}\Delta M$ [17] we can readily obtain

$$\frac{\delta_l}{\eta_{min}} \approx \frac{M_t}{\Delta M} R_\lambda{}^{\beta} \tag{23}$$

where $\beta = (3/2)(1-\alpha_{min})/(3+\alpha_{min}) - 1/2$. While extremely difficult to measure, α_{min} may not be too far from zero [53]. In such a case $\beta = 0$, and therefore,

$$\frac{\delta_l}{\eta_{min}} \approx \frac{M_t}{\Delta M}. \tag{24}$$

This result suggests that, as a consequences of the intermittency in the quasi-singular dissipation field, scales much smaller that the mean Kolmogorov scale can be of the order of the shock thickness if $M_t/\Delta M$ is not too small. In such a case, the interaction between small-scale turbulence and the shock can lead effectively to a broken regime. The scaling with the parameter $M_t/\Delta M$ is consistent with the estimates in Sec. 3 based on velocity gradients.

6. Conclusions

We have investigated the relation between small-scale intermittency and shocks in turbulent flows. Since both turbulence and shock gradients become stronger at high Reynolds number, it is important from a fundamental as well as practical perspective to understand whether intermittent turbulence gradients can be as strong as shocks in compressible flows and have a sizable (even disruptive) effect on, for example, the shock structure in shock-turbulence interactions. To assess this possibility we have considered the interaction of isotropic turbulence with a normal shock, a configuration where it has indeed been observed that under certain conditions, turbulence can produce local topological changes in the otherwise well-defined shock surface leading to “holes” in the shock. When the interaction leads to such a phenomenon the interaction is said to be in the “broken” regime.

Our main result is based on the comparison of turbulent and shock gradients. In particular we introduced the parameter K_u defined as the ratio of most intense turbulence gradient and the largest gradient at the shock. While the latter can be easily estimated using classical solutions of Navier-Stokes equations in the low Mach number limit, the former presents more challenges. In order to estimate the turbulence gradients we consider two theoretical approaches (Yakhot and Sreenivasan [37] and the multifracal formalism [36]), which relate moments of the most intense turbulence gradients with widely studied scaling exponents of structure functions ζ_n in the inertial range. The most intense gradients are shown to be related to the asymptotic form of ζ_n at large n.

For non-intermittent turbulence, we have shown that as the Reynolds number increases the shock gradient becomes stronger compared to gradients in the incoming turbulence. However, for more realistic intermittent turbulence with scaling exponents ζ_n that grow more slowly than linear in n, the Reynolds number dependence disappear. The parameter K_u is then simply given by $K_u = {M_t}^2/\Delta M^2$ which shows that for real life applications, turbulence gradients are comparable to the shock. This result is also consistent with our analysis of the length scales involved in the problem using the multifractal description of turbulence. We have shown that the ratio of the shock thickness with the smallest scale (associated with the most singular fluctuations of the dissipation rate) scales as $M_t/\Delta M$.

Our results, thus, suggest that strong intermittent (positive) gradients in the incoming turbulence may counteract the (negative) shock gradient in such a way to create holes and, therefore, a broken shock. Using our DNS database of incompressible and compressible turbulence, we have further shown that strong gradients are correlated with lower velocities. Thus, the strongest turbulence gradients will interact with a lower-Mach number (weaker) shock making this a plausible mechanism for broken shocks. This result is consistent with recent work [17] suggesting flow retardation ahead of the shock was related to broken shocks. In that reference, the parameter $M_t/\Delta M$ is also suggested to control the regime of the interaction, consistent with our results.

References

[1] Sreenivasan KR. Fluid turbulence. Rev Mod Phys. 1999;71:S383–S395.

[2] Sreenivasan KR, Antonia RA. The phenomenology of small-scale turbulence. Annu Rev Fluid Mech. 1997;29:435–472.

[3] Porter D, Pouquet A, Sytine I, Woodward P. Turbulence in compressible flows. Physica A. 1999;263:263–270.

[4] Porter D, Pouquet A, Woodward P. Measures of intermittency in driven supersonic flows. Phys Rev E. 2002;66:026301.

[5] Pan L, Padoan P, Kritsuk AG. Dissipative structures in supersonic turbulence. Phys Rev Lett. 2009;102.

[6] Lee S, Lele SK, Moin P. Eddy shocklets in decaying compressible turbulence. Phys Fluids. 1991;3:657–664.

[7] Samtaney R, Pullin DI, Kosovic B. Direct numerical simulation of decaying compressible turbulence and shocklet statistics. Phys Fluids. 2001;13:1415.

[8] Pirozzoli S, Grasso F. Direct numerical simulations of isotropic compressible turbulence: Influence of compressibility on dynamics and structures. Phys Fluids. 2004;16:4386 – 4407.

[9] Andreopoulos Y, Agui JH, Briassulis G. Shock wave-turbulence interactions. Annu Rev Fluid Mech. 2000;32:309–345.

[10] Ribner HS. Shock-turbulence interaction and the generation of noise. NACA TN-3255. 1954;.

[11] Ribner HS. Convection of a pattern of vorticity through a shock wave. NACA TR-1164. 1954;.

[12] Moore FK. Unsteady oblique interaction of a shock wave with a plane disturbance. NACA Report 1165; 1954.

[13] Truesdell C. On curved shocks in steady plane flow of an ideal fluid. J Aeronaut Sci. 1952;19(12):826–828.

[14] Hayes WD. The vorticity jump across a gasdynamic discontinuity. J Fluid Mech. 1957;2:595–600.

[15] Jacquin L, Cambon C, Blin E. Turbulence amplification by a shock wave and rapid distortion theory. Phys Fluids. 1993;5:2539–2550.

[16] Wouchuk JG, de Lira CHR, Velikovich AL. Analytical linear theory for the interaction of a planar shock wave with an isotropic turbulent vorticity field. Phys Rev E. 2009;79:066315.

[17] Donzis DA. Shock structure in shock-turbulence interactions. Phys Fluids. 2012;p. (accepted).

[18] Lee S, Lele SK, Moin P. Direct numerical simulation of isotropic turbulence interacting with a weak shock wave. J Fluid Mech. 1993;251:533–562.

[19] Lee S, Lele SK, Moin P. Interaction of isotropic turbulence with shock waves: effect of shock strength. J Fluid Mech. 1997;340:225–247.

[20] Jamme S, Cazalbou JB, Torres F, Chassaing P. Direct Numerical Simulation of the Interaction between a Shock Wave and Various Types of Isotropic Turbulence. Flow, Turb Comb. 2002;68:227–268.

[21] Larsson J, Lele SK. Direct numerical simulation of canonical shock/turbulence interaction. Phys of Fluids. 2009;21:126101.

[22] Honkan A, Andreopoulos J. Rapid compression of grid-generated turbulence by a moving shock-wave. Phys Fluids. 1992 Nov;4(11):2562–2572.

[23] Honkan A, Watkins CB, Andreopoulos J. Experimental-study of Interactions of Shock-wave With Free-stream Turbulence. J Fluids Eng. 1994 Dec;116(4):763–769.

[24] Briassulis G, Andreopoulos J. High resolution measurements of isotropic turbulence interacting with shock waves. AIAA Paper. 1996;96:0042.

[25] Agui JH, Briassulis G, Andreopoulos Y. Studies of interactions of a propagating shock wave with decaying grid turbulence: velocity and vorticity fields. J Fluid Mech. 2005;524:143–195.

[26] Donzis DA. Amplification factors in shock-turbulence interactions: effect of shock thickness. Phys Fluids. 2012;24:011705.

[27] Hesselink L, Sturtevant B. Propagation of weak shocks through a random medium. J Fluid Mech. 1988;196:513–553.

[28] Donzis DA, Yeung PK, Sreenivasan KR. Dissipation and enstrophy in isotropic turbulence: scaling and resolution effects in direct numerical simulations. Phys Fluids. 2008;20:045108.

[29] Frisch U. Turbulence. Cambridge University Press; 1995.

[30] Thompson PA. Compressible Fluid Dynamics. New York: McGraw Hill; 1984.

[31] Alsmeyer H. Density profiles in argon and nitrogen shock waves measured by the absorption of an electron beam. J Fluid Mech. 1976;74:497–513.

[32] Garca-Coln LS, Velasco RM, Uribe FJ. Beyond the Navier-Stokes equations: Burnett hydrodynamics. Phys Reports. 2008 Aug;465(4):149–189.

[33] Elizarova TG, Khokhlov AA, Montero S. Numerical simulation of shock wave structure in nitrogen. Phys Fluids. 2007;19.

[34] Greenshields CJ, Reese JM. The structure of shock waves as a test of Brenner's modifications to the Navier-Stokes equations. J Fluid Mech. 2007;580:407–429.

[35] Taylor GI. The conditions necessary for discontinuous motion in gases. Proc R Soc Lond A. 1910;84:371–377.

[36] Nelkin M. Multifractal scaling of velocity derivatives in turbulence. Phys Rev A. 1990;42:7226–7229.

[37] Yakhot V, Sreenivasan KR. Towards a dynamical theory of multifractals in turbulence. Physica A. 2004;343:147–155.

[38] Yakhot V, Sreenivasan KR. Anomalous scaling of structure functions and dynamic constraints on turbulence simulations. J Stat Phys. 2005;121:823–841.

[39] Van Atta CW, Antonia RA. Reynolds-number dependence of skewness and flatness factors of turbulent velocity derivatives. Phys Fluids. 1980;23:252–257.

[40] Wyngaard JC, Tennekes H. Measurements of small-scale structure of turbulence at moderate Rreynolds numbers. Phys Fluids. 1970;13:1962.

[41] Schumacher J, Sreenivasan KR, Yakhot V. Asymptotic exponents from low-Reynolds-number flows. New J Phys. 2007;9:89.

[42] Sreenivasan KR. An update on the energy dissipation rate in isotropic turbulence. Phys Fluids. 1998;10:528–529.

[43] She ZS, Leveque E. Universal scaling laws in fully developed turbulence. Phys Rev Lett. 1994;72:336–339.

[44] Kolmogorov AN. Local structure of turbulence in an incompressible fluid for very large Reynolds numbers. Dokl Akad Nauk SSSR. 1941;30:299–303.

[45] Novikov EA. Infinitely divisible distributions in turbulence. Phys Rev E. 1994;50:R3303–R3305.

[46] Yakhot V. Mean-field approximation and a small parameter in turbulence theory. Phys Rev E. 2001;63:026307.

[47] Nelkin M. Inertial range scaling of intense events in turbulence. Phys Rev E. 1995;52:R4610–R4611.

[48] Benzi R, Biferale L, Fisher RT, Kadanoff LP, Lamb DQ, Toschi F. Intermittency and Universality in Fully Developed Inviscid and Weakly Compressible Turbulent Flows. Phys Rev Lett. 2008;100:234503.

[49] Monin AS, Yaglom AM. Statistical Fluid Mechanics. vol. 2. MIT Press; 1975.

[50] Kailasnath P, Sreenivasan KR. Zero crossings of velocity fluctuations in turbulent boundary-layers. Phys Fluids. 1993;5:2879–2885.

[51] Sreenivasan KR, Bershadskii A. Clustering properties in turbulent signals. J Stat Phys. 2006;125:1145–1157.

[52] Sreenivasan KR, Meneveau C. Singularities of the equations of fluid motion. Phys Rev A. 1988;38:6287–6295.

[53] Sreenivasan KR. Possible effects of small-scale intermittency in turbulent reacting flows. Flow, Turb Comb. 2004;72:115–131.